Journal of Applied Mathematics and Physics, 2013, 1, 4-8
http://dx.doi.org/10.4236/jamp.2013.12002 Published Online May 2013 (http://www.scirp.org/journal/jamp)

The Synthesis and Characterization of Arc Melted $Fe_{1-x}Al_x$ Alloys

Sandeep Rajan[1*], Rajni Shukla[1], Anil Kumar[2], Anupam Vyas[2], Ranjeet Kumar Brajpuriya[2]
[1]Department of Physics, Deenbandhu Chhotu Ram University of Science & Technology, Sonipat, India
[2]Department of Physics, Amity University Haryana, Gurgaon, India
Email: *search.rajain@gmail.com

Received May 10, 2013; revised June 11, 2013; accepted June 17, 2013

Copyright © 2013 Sandeep Rajan *et al*. This is an open access article distributed under the Creative Commons Attribution License, which permits unrestricted use, distribution, and reproduction in any medium, provided the original work is properly cited.

ABSTRACT

The paper presents correlation study on a series of $Fe_{1-x}Al_x$ alloy samples prepared by arc melting. All the samples show crystalline structure, irrespective of the Al content and are textured mainly along (110) direction. The particle size decreases rapidly with x particularly after $x > 0.3$. The corresponding magnetic measurements were obtained at room temperature using a VSM, with a maximum applied field of 14 kOe. The results show that the ferromagnetic state of the samples disappears with x, and becomes paramagnetic for alloys with $x \geq 0.4$. It is also found that coercivity (H_c) and resistivity increase with x. The results were interpreted in terms of continuous change in their electronic structure *i.e.* overlap of the electron wave functions of the magnetic atoms with the Al electron wave function.

Keywords: Transition Metal Aluminides; Magnetization and Electronic Properties

1. Introduction

During the last decade, enormous progress has been made in manufacturing and processing of materials with intermetallic matrices [1]. Mechanical alloying (MA) [2], which was initially conceived for the production of dispersion strengthened superalloys, is nowadays used for synthesizing a wide range of materials including intermetallics [3]. A great advantage of mechanical alloying (MA) process is the fact that it modifies the structure and solid solubility limits of alloys and solid solutions and induces lattice strains and phase transformations [4,5]. The formation of metastable phases and disordering of the lattice through alloying gives rise to interesting mechanical and magnetic properties [6]. This is particularly evident in the case of Fe-Al intermetallic systems. The complicated phase diagram and the dependence of magnetic properties on the state of disorder and the microstructure [6,7] make this an interesting system to study through the MA process. Both from the point of view of understanding the collective behaviour of the magnetic phases and also possible applications, study of such intermediate phases is expected to be very rewarding. As FeAl intermetallic compound offers a combination of several attractive properties such as a high specific strength, good strength at intermediate temperatures and an excellent corrosion resistance at elevated temperatures under oxidizing, carburing and sulfidizing atmospheres [8,9]. So they have attracted considerable attention as potential candidates for structural and coatings applications at elevated temperatures in hostile environments and as promising substitutes for stainless steels at room temperature [10-13]. Due to these reasons, mechanically alloyed [3-5] and mechanically milled [14] Fe-Al systems of various compositions have been investigated in recent years. With this objective, the authors have successfully synthesized FeAl intermetallics by MA and systematically investigated the structural, magnetic and electronic properties of a series of arc melted $Fe_{1-x}Al_x$ ($0.2 \leq x \leq 0.6$) alloys using XRD, VSM and XPS.

2. Experimental Details

A series of arc melted $Fe_{1-x}Al_x$ alloy samples were prepared under Argon atmosphere using high purity (more than 99.9%) constituent's metals. Afterwards, the polycrystalline ingots were annealed at 600˚C for 120 hr under the UHV condition.

The structure, average grain size and lattice constant a_0 of each sample was inferred from the X-ray diffraction (XRD). In the present study, the average crystallite size <L> was calculated from the broadening of XRD peaks

*Corresponding author.

according to Scherrer's formula

$$< L >= \frac{k\lambda}{\beta_L \cos\theta}$$

where k represented the shape factor which varied with the crystal shape, λ is the wavelength of the CuKα radiation, θ is the Bragg angle, and β_L is the Lorentzian part of the integral breadth due to the crystallite size.

The lattice parameter calculated using the equation

$$\frac{4\sin^2\theta}{\lambda^2} = \frac{h^2+k^2+l^2}{a_0^2}$$

The corresponding magnetic and resistivity measurements were done using vibrating sample magnetometer and standard four-probe resistivity method. The chemical and electronic information of the samples at different depth has been obtained from XPS technique. X-ray photoelectron spectroscopy (XPS) study was carried out at a base pressure better than 5×10^{-9} Torr. Hereafter, for simplicity we have named the sample $Fe_{80}Al_{20}$ (x = 0.2) as Sample A, $Fe_{70}Al_{30}$ (x = 0.3) as Sample B, $Fe_{60}Al_{40}$ (x = 0.4) as Sample C, $Fe_{50}Al_{50}$ (x = 0.5) as Sample D and $Fe_{40}Al_{60}$ (x = 0.6) as Sample E.

3. Results and Discussion

Figure 1 displays the XRD patterns of $Fe_{1-x}Al_x$ ($0.2 \le x \le 0.6$) samples as a function of x. Only a narrow range of diffraction angles is presented (2θ =25˚ - 55˚), but it contains the main lines of all components and is representative of the evolution that occurs. All the samples show crystalline structure and textured mainly along (110) direction, irrespective of the Al content. **Figure 1(a)** shows the diffraction pattern of sample A ($Fe_{80}Al_{20}$). The peak at 31.04˚ can be attributed to a new phase which possesses the same structure type as the bcc Fe (Al). The peak at 2θ = 39.3˚ of Al (111) is absent shows complete

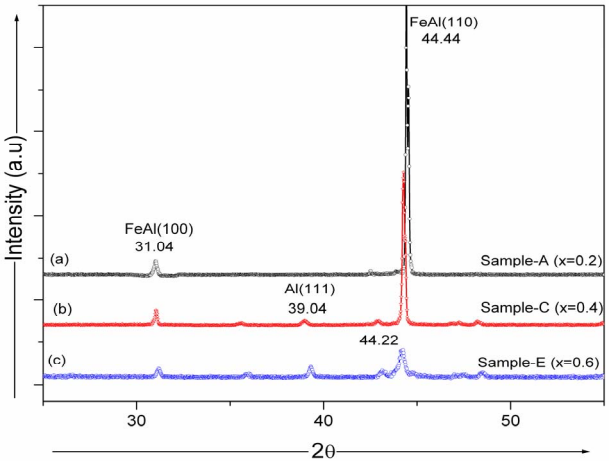

Figure 1. XRD patterns of $Fe_{1-x}Al_x$ samples as a function of x.

dissolution of Al with Fe, which further supports the formation of Fe (Al) solid solution. Further, it is seen that the fundamental peaks are consistently broadened and shifted to lower angles with increase in x. The broadening of the peaks is due to the rapid reduction in average crystallite size and an increase in lattice strain. It is found that that average crystallite size decreases rapidly with x particularly after x > 0.3 (see **Table 1**). The shifting of the fundamental peaks to lower angles indicates an expansion of the lattice and presence of internal strain occurs as a result of non-uniform alloy formation during sample preparation. The variation in lattice parameter (a_0) as a function of Al content is shown in **Table 1**. This can be understood if we take into account that the Al atoms enter the Fe lattice producing a local dilatation due to their larger size.

The diffraction pattern of Sample C shows some marked differences. In addition to reduction in peak intensity and shift in peak position, a small peak at 39.04˚ corresponds to Al (111) is also present in the pattern indicating that whole Al does not mix completely with Fe to form uniform FeAl alloy. As already mentioned, Arc melting process is a non-equilibrium process and has no sufficient time to form stable and ordered phases, so meta-stable and disordered phases will be formed. Further considerable reduction in the peak intensity of Samples D and E with x clearly indicates the structural transformation and formation of Al rich FeAl phases. The average crystallite size in these cases are reduces drastically to 28 nm and 26 nm, respectively. After seeing the results one may expect the formation of an off stoichiometric Fe_3Al phase in the Fe-rich samples, while the Al-rich compositions have both Al-rich phases and clustering of Fe and Al atoms, respectively.

The corresponding hysteresis loops M (H) for all the samples were obtained at room temperature using a VSM, with a maximum applied field of 14 kOe (see **Figure 2**). From the inset of **Figure 2(a)** it is clearly seen that Sample A show saturation with applied magnetic field indicating the ferromagnetic nature of the sample with a strong anisotropy leading to in plane easy direction of the

Table 1. Parameters obtained from XRD and VSM data analysis for $Fe_{1-x}Al_x$ alloy samples as a function of x.

Parameter / Composition	L (nm)	a_0 (Å)	ρ (μΩcm)	H_c (Oe)	Ms (emu)
x = 0.2	116	2.879	93	1.7	3.22
x = 0.3	111	2.883	117	2.9	1.88
x = 0.4	78	2.889	178	33.3	0.81
x = 0.5	28	2.894	165	71.7	0.045
x = 0.6	26	2.894	144	46.4	0.0046

Copyright © 2013 SciRes.

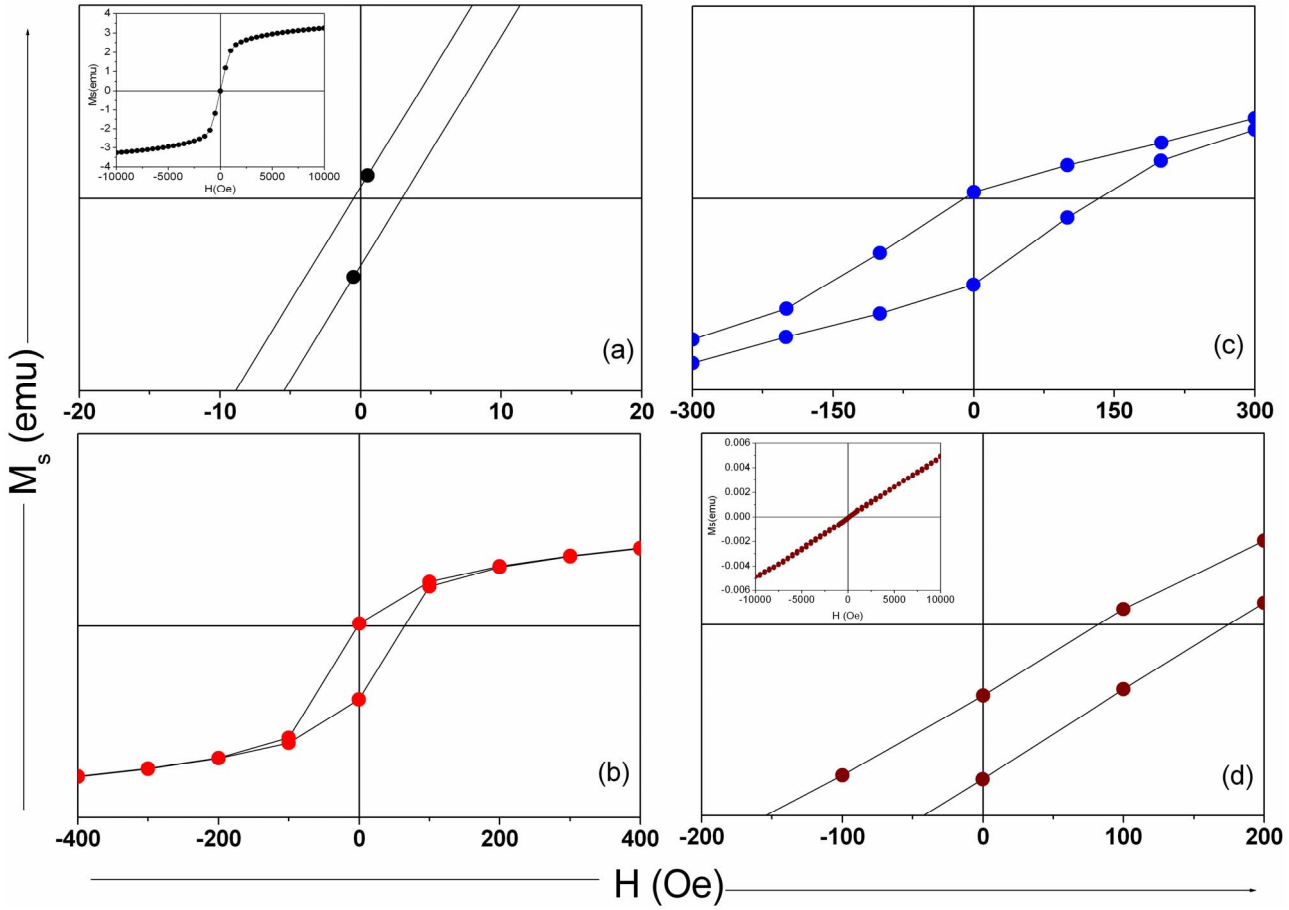

Figure 2. M-H curves of $Fe_{1-x}Al_x$ samples as a function of x, (a) Sample A; (b) Sample C; (c) Sample D; and (d) Sample E.

magnetization. However, magnetization and room temperature ferromagnetic state gradually disappears with increasing x, up to $x \leq 0.3$. On further increasing x, the ferromagnetic state disappears more rapidly, becoming paramagnetic for alloys with $x \geq 0.4$. The samples with high Al content ($x \geq 0.4$) do not show saturation even after applying the maximum applied field of 14 kOe. This characteristic reflects the gradual development of alloying process of Fe with Al. Al reduces the direct ferromagnetic interaction between Fe-Fe sites and at the same time increase in anti-ferromagnetic interaction could takes place, which reduces the magnetic moment of Fe. Further, there is also a shift in the hysteresis loop indicating of moment pinning due to highly disordered and non-uniform nature of the sample. This loop shift can be explained as originating from the phenomena of exchange bias [15] associated with the exchange anisotropy created at the interface between AFM-FM phases. It is also found that coercivity (H_c) increases with x (from ~1.7 Oe to ~71.7 Oe), see **Table 1**. The increase of H_c with the decreasing particle size may indicate that pinning at the grain boundaries may be important origin of the coercivity; indeed smaller grain size corresponds to larger number of grain boundaries results enhancement in the anisotropy which act as barriers to the motion of the domain walls, increasing thus the coercive field. **Table 1** also shows the saturation magnetization value of the $Fe_{1-x}Al_x$ samples as a function of x. The progressive decrease of the saturation magnetization is attributed to competition between nearest neighbour Fe-Fe ferromagnetic exchange and an indirect FeAl anti-ferromagnetic interaction and the alloy become nonmagnetic around 0.5% Al. The system can be considered to be consisting of a ferromagnetic phase dispersed in a non-magnetic medium. The presence of spontaneous magnetization in the system indicates that the magnetic grains are coupled through exchange interactions. The exchange interaction can be a Ruderman Kittele Kasuyae Yosida (RKKY) type of interaction mediated by the itinerant electrons present in the system or through a super-exchange type of interaction due to the overlap of the electron wave functions of the magnetic atoms with the Al electron wave functions.

The value electrical resistivity of $Fe_{1-x}Al_x$ samples as a function of x is shown in **Table 1**. It is seen that the resistivity increases sharply with increase in x and show a

Copyright © 2013 SciRes.

maximum value of 178 μΩcm at x = 0.4. The resistivity initially increases with concentration as it should since increasing disorder, brought about by rising Al concentration, contributes to increasing electron scattering. In addition, the formation of different phases of FeAl is responsible for high value of resistivity. Further increase of Al yields a steep decrease in the electrical resistivity, and the resistivity of the FeAl alloy containing 60 at.% Al approaches a value of 144 μΩcm. It is easy to understand from the electronic structure of Fe and Al atoms that 3s orbitals of Al are very close in energy to the 3d orbitals of Fe, thus providing the grounds for a strong overlap between Fe-3d and Al-3s as these elements are alloyed. But important to note that the 3p electrons of Al lie at an energy higher than the 3d and 4s electrons of Fe. Thus, as these elements are alloyed, one would expect a charge transfer from Al-3p to Fe-3d, as the 4s orbitals of Fe are full and this charge transfer affect the resistivity as well as magnetic moment of Fe due to filling of the 3d orbitals. Further addition of Al above 40 at.% value essentially adds more electrons to a nearly free electron conduction band and the resistivity falls sharply.

Figure 3 shows the core level and valence band (VB) spectra of Sample B and D recorded after 90 min of sputtering. The recorded spectrum of Fe and Al shows some significant differences, which are characteristics of the oxidized state (see **Figures 3(a)** and **(b)**). The Fe-2p spectrum is split by the 2p-spin–orbit effect into the $2p_{3/2}$ and $2p_{1/2}$ regions and continuous tail is caused by electron-hole pair excitations and is a signature of the metallic states. Similarly, the set of typical Al-2p spectra consist of spin orbit doublet peaks corresponding to Al-$2P_{3/2}$ and Al-$2p_{1/2}$ level states.

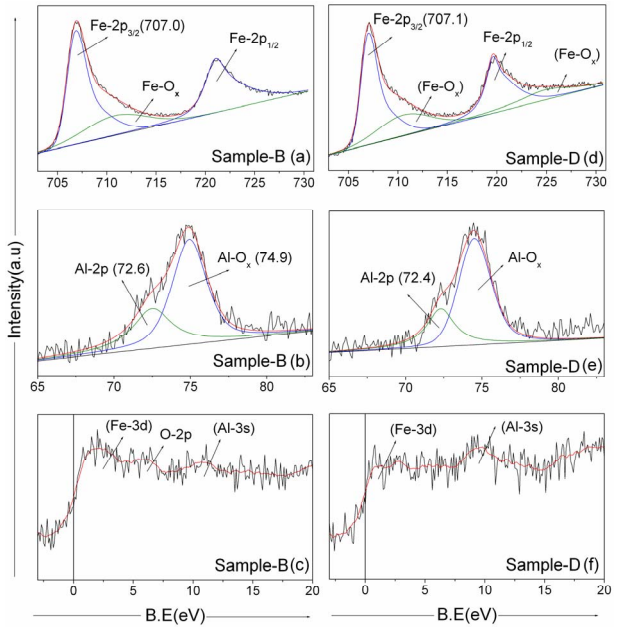

Figure 3. Fe-2p, Al-2p core levels and VB spectra of Sample B and Sample D recorded after 90 min sputtering.

However, spectrometer resolution (0.8 eV) does not allow distinction of their structure. Another important point is that the relative intensity of Al-O_x peak is higher than pure Al-2p peak indicating that oxygen is mainly reacted with Al and partially with Fe (see **Figures 3(a)** and **(b)**). The corresponding VB spectra show three distinct features; a broad Fe-3d band around 2.3 eV near the Fermi level and other broad band lying deeper in energy at 6.3 eV are attributed to π and σ molecular orbitals, respectively formed by the hybridization of Al-3sp and O-2p orbitals and Al-3s band at 10.8 eV (see **Figure 3(c)**). However in case of sample D, Fe-$2P_{3/2}$ peak is observed at 707.1 eV and is shifted by 0.3 eV towards higher binding energy and Al-2p peak by 0.35 eV but towards lower binding energy as compared to their elemental Fe-2p and Al-2p core line (see **Figures 3(d)** and **(e)**).

If we compare Samples B and D, we find some differences in the binding energy positions of Fe-2p and Al-2p core lines. The binding energy of the Fe-2p peaks is shifted towards higher binding energy and Al-2p towards lower binding energy as compared to their element peak position; also the shift in Sample B is different from Sample D. The different shift in each case is due to the formation of different phases of FeAl, *i.e.* Fe rich in Sample B and Al rich in Sample D. Further in the VB spectra of Sample D, one can see apart from 3d photoemission band of Fe at 1.8 eV, strong feature around 9.6 eV is also observed corresponding to Al-3s as is very small in case of Sample B. Due to this, Fe-3d density of states (DOS) are drastically modified and the emission band is shifted towards lower binding energy *i.e.* towards Fermi level. This is due to the strong hybridization of sp-d states at Fermi level as a result of charge transfer from valance Al-3p and 3s electrons to minority 3d orbital of Fe. Our results were matches well with the earlier theoretical results.

4. Conclusion

The results conclude the formation of an off stoichiometric Fe_3Al phase in Fe-rich samples, while the Al-rich compositions have both Al-rich phases and clustering of Fe and Al atoms The corresponding magnetic measurements show decrease in saturation magnetization and increase in resistivity with x and is attributed to dilution of Fe moment in the Al rich compositions due to sp-d hybridization.

REFERENCES

[1] G. Sauthoff, "State of Intermetallics Development," *Ma-*

Copyright © 2013 SciRes.

terials and Corrosion, Vol. 47, No. 11, 1996, pp. 589-594. doi:10.1002/maco.19960471103

[2] H. W. Sheng, Y. H. Zhao, Z. Q. Hu and K. Lu, "Lattice Instability in the Solid State Amorphization of Fe(Al) Solid Solution by Mechanical Alloying," *Physical Review B*, Vol. 56, No. 5, 1997, pp. 2302-2305. doi:10.1103/PhysRevB.56.2302

[3] Q. Zeng and I. Baker, "Magnetic Properties and Thermal Ordering of Mechanically Alloyed Fe-40 at.% Al," *Intermetallics*, Vol. 14, No. 4, 2006, pp. 396-405.

[4] M. Krasnowsky and T. Kulik, "Nanocrystalline FeAl Intermetallic Produced by Mechanical Alloying Followed by Hot-Pressing Consolidation," *Intermetallics*, Vol. 15 No. 2, 2007, pp. 201-205. doi:10.1016/j.intermet.2006.05.008

[5] P. Pochet, E. Tominez, L. Chaffron and G. Martin, "Order-Disorder Transformation in Fe-Al under Ball Milling," *Physical Review B*, Vol. 52, No. 6, 1995, pp. 4006-4016. doi:10.1103/PhysRevB.52.4006

[6] A. Hernando, X. Amils, J. Nogues, S. Surinach, M. D. Baro and M. R. Ibarra, "Influence of Magnetization on the Reordering of Nanostructured Ball-Milled Fe-40 at.% Al Powders," *Physical Review B*: *Condensed Matter and Materials Physics*, Vol. 58, No. 18, 1998, pp. R11864-R11867. doi:10.1103/PhysRevB.58.R11864

[7] E. Apinaniz, F. Plazaola, J. S. Garitaonandia, D. Martin and J. A. Jimenez, "Study of the Enhancement of the Magnetic Properties of $Fe_{70}Al_{30}$ in the Order-Disorder Transition," *Journal of Applied Physics*, Vol. 93, No. 10, 2003, pp. 7649-7651. doi:10.1063/1.1544504

[8] I. Baker and E. P. George, In: S. C. Deevi and V. Sikka, Eds., *Aluminides*: *Processing Properties and the Mechanical Properties of FeAl*, *Proceedings of the International Symposium on Nickel and Iron Aluminides*: *Processing*, *Properties and Applications*, The Metallurgical Society, Warrendale, 1997, pp. 145-156.

[9] P. F. Tortorelli and J. H. DeVan, "Behavior of Iron Aluminides in Oxidizing/Sulfidizing Environments," *Materials Science and Engineering A*, Vol. 153, No. 1-2, 1992, pp. 573-577. doi:10.1016/0921-5093(92)90253-W

[10] S. C. Deevi, V. K. Sikka and C. T. Liu, "Processing, Properties and Applications of Nickiel and Iron Aluminides," *Progress in Materials Science*, Vol. 42, No. 1-4, 1997, pp. 177-192. doi:10.1016/S0079-6425(97)00014-5

[11] N. S. Stoloff, "Iron Aluminides: Present Status and Future Prospects," *Materials Science and Engineering A*, Vol. 258, No. 1-2, 1998, pp. 1-14. doi:10.1016/S0921-5093(98)00909-5

[12] C. T. Liu, E. P. George, P. L. Maziasz and J. H. Schneffiel, "Recent Advances in B2 Iron Aluminide Alloys: Deformation, Fracture and Alloy Design," *Materials Science and Engineering* A, Vol. 258, No. 1-2, 1998, pp. 84-98.

[13] Q. Zeng and I. Baker, "Magnetic Properties and Thermal Ordering of Mechanically Alloyed Fe-40 at% Al," *Intermetallics*, Vol. 14, No. 4, 2006, pp. 396-405. doi:10.1016/j.intermet.2005.07.005

[14] L. F. Kiss, D. Kaptas, J. Balogh, L. Bujdoso, T. Kemeny and L. Vincze, "Rigid Magnetic Foam-Like Behavior in Ball-Milled FeAl," *Physical Review B*, Vol. 70, 2004, Article ID: 012408. doi:10.1103/PhysRevB.70.012408

[15] J. Nogues and I. K. Schuller, "Exchange Bias," *Journal of Magnetism and Magnetic Materials*, Vol. 192, No. 2, 1999, pp. 203-232. doi:10.1016/S0304-8853(98)00266-2

Copyright © 2013 SciRes.